Irradiation effects in tungsten - from surface effects to bulk mechanical properties

J. Riesch¹, A. Feichtmayer^{1,2}, J.W. Coenen³, B. Curzadd^{1,2}, T. Höschen¹, A. Manhard¹, T. Schwarz-Selinger¹, R. Neu^{1,2}

- ¹ Max-Planck-Institut für Plasmaphysik, 85748 Garching, Germany
- ² Technische Universität München, 85748 Garching, Germany
- ³ Forschungszentrum Jülich GmbH, Institut für Energie- und Klimaforschung Plasmaphysik, 52425 Jülich, Germany

E-mail: johann.riesch@ipp.mpg.de

Abstract. Advanced materials as tungsten fibre reinforced composites allow to overcome severe weaknesses of the standard materials for plasma facing components copper and tungsten. The effect of the fusion environment on the mechanical properties of these materials, e.g. the embrittlement by neutron irradiation, plays a key role for the development of future fusion reactors. To simulate this effect high-energy ions are used as a substitute for the displacement damage by neutrons. We propose the use of very fine tungsten wire as a possibility of studying the influence of irradiation damage on the mechanical properties as they allow a full-depth irradiation despite the limited penetration depth of these ions. Geometrical size effects are mitigated due to the nanoscale microstructure of the wires. In addition, as such wires are used in tungsten fibre-reinforced composites the investigation of irradiated wires allows the prediction of the bulk composite properties. For the proof of this concept tungsten wire with a diameter of $16\,\mu\mathrm{m}$ was thinned to $5\,\mu\mathrm{m}$ and irradiated with $20.5\,\mathrm{MeV}~\mathrm{W}^{6+}$ ions. The mechanical properties were subsequently determined by macroscopic tensile testing. Irradiation to 0.3 dpa, 1 dpa and 9 dpa did not lead to a change of the mechanical behaviour. Both strength and ductility, the latter indicated by the reduction of area, were similar to the as-fabricated state.

Keywords: tungsten, fibre, ion irradiation, embrittlement, tension test, ductility

1. Introduction

10

15

20

25

For next step fusion reactors like DEMO [1] or a fusion power plant the requirements for first wall materials will be more stringent than for current devices and will lead to the need of advanced materials [2, 3]. Favourite candidate materials like tungsten (W) for the plasma facing parts and copper (Cu) for cooling structures have severe weaknesses. Tungsten is brittle at low temperature and susceptible to embrittlement by thermal overload [4] and/or irradiation [5, 6]. In the case of copper the strength is strongly reduced above 300 °C [7]. A promising way to improve upon the properties of

conventional materials is reinforcement with high-strength ductile drawn W wire [8]. By using potassium doped tungsten wire these preferential properties are preserved up to very high temperatures [9]. In tungsten fibre-reinforced tungsten composites (W_f/W) the fibres are embedded in a W matrix produced by powder metallurgy or a chemical vapour deposition process. An engineered interface between fibre and matrix, e.g. a thin oxide layer, allow controlled deflection of growing cracks. By this energy dissipating mechanisms allowing the relaxation of stress peaks are activated and the resistance to fracture is increased [10, 11] similar as in ceramic fibre-reinforced ceramics (see e.g. [12]). Tungsten wire is also used to reinforce copper materials in order to improve their strength at elevated temperature [13]. W and Cu combine very well as they form a strong bond without forming a solid solution [14].

In a future fusion reactor high neutron fluxes originating from the D-T nuclear reaction will occur [15]. The impinging neutrons will cause displacement damage and transmutation, leading to a significant change in material properties. Exposure of metals to irradiation in general leads to an increase in strength accompanied by a decrease of ductility [16]. This behaviour is known as irradiation hardening and can lead to a complete loss of ductility in bcc metals. The reason for this hardening is the production of various defects in the lattice. Beside the change in mechanical properties, an increase in the uptake and retention of hydrogen are of concern [17]. In a fusion reactor the materials are subjected to a very specific energy spectrum of neutrons going up to an energy of 14 MeV (see e.g. [18]). At the moment, there is no facility available to test under these conditions. Alternatively, two methods are used to simulate the effect: neutron irradiation in a fission reactor and irradiation by high energetic ions. Although fission can be readily used [19] there are concerns about the differences in the energy spectrum [20]. Due to the need of long irradiation times and the activation of samples the costs and cycle times (from outlining experiments until receiving results) are very high [16]. On the other hand, the use of ion beams allows fast iterations which are very helpful in material development programs. Here, the damage created by heavy ions is very similar to neutron induced damage [16]. The conditions during ion irradiation are well controllable allowing defined energies, dose rates and temperatures [21]. Furthermore it allows very high dose rates up to $10 \,\mathrm{dpa}\,\mathrm{h}^{-1}$ when using heavy ions (for comparison, dose rates in fission reactors are in the range of 1 dpa year⁻¹ [22]). Compared to neutron irradiation the activation of the samples is little which makes post testing and characterisation easier (no hot cells required). By using self-ion irradiation, i.a. the damaging ion is the same material as the damaged material, the implantation of impurities is avoided. In contrast to neutron irradiation no transmutation occurs for heavy ions. A large drawback for the study of structural material is the shallow penetration depth of a few nm to approximately 100 µm (for light ions). For 20.5 MeV W^{6+} ions the damaging zone reaches depths of up to $2.5\,\mu m$ with a peak at around 1.3 µm as calculated by SRIM [23] (profile is e.g. given in [24]). A comprehensive overview about the use of ion irradiation as a substitute for neutron irradiation is given by Was et al. [21, 16].

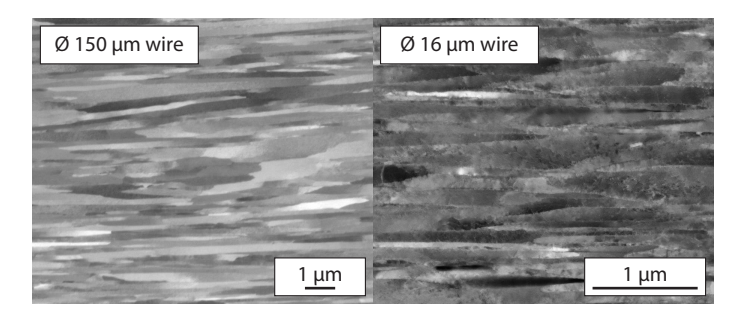


Figure 1. Scanning electron microscopy (SEM) pictures of the longitudinal section of tungsten wire with a diameter of $150 \,\mu\text{m}$ (left) and $16 \,\mu\text{m}$ (right) (Z contrast using the circular backscatter detector (CBS) detector. Both sections were prepared by a focussed ion beam polishing within the SEM. The magnifications are chosen to show similar sizes for the grains but note the differences in the scale bars.

As a consequence of the shallow penetration depth, the mechanical properties are frequently investigated by nano indentation or micro mechanical testing [25]. During nano indentation the affected volume is typically larger than the irradiation depth which makes the determination of the irradiation effect and the mechanical properties difficult [26]. In micro mechanical testing the actual sample size is often in the same length scale as the microstructural features and thus the results represent the properties of these features rather than that of the bulk material. The extrapolation of the results to bulk material behaviour is often challenging due to this size effect [27].

In this contribution fine grained tungsten wire is proposed as a polycrystalline model system to avoid this problem. We assess the mechanical properties after ion irradiation by tensile testing to investigate ductility and strength directly. The first results of irradiation by W^{6+} up to 9.5 dpa are presented.

2. Tungsten wire - a polycrystalline model system

Tungsten wire is produced by multi step drawing. The large deformation leads to a very fine microstructure. In figure 1 the longitudinal sections of a tungsten wire with a diameter of 150 µm (left) as frequently used in W_f/W composites and of a wire with a diameter of 16 µm (right) are shown. Especially the grain size of the 16 µm wire is so small that even within the damage range of heavy ions many grains are in the affected volume. In [28] it was shown that wires with diameters of 150 µm and 16 µm which was electrochemically thinned to 5 µm show very similar tensile behaviour and ductility (considering the reduction in area as the characteristic property). Assuming a penetration depth of 2.5 µm for 20.5 MeV W^{6+} ions and irradiation from two opposite sites it would be possible to irradiate the full volume of 5 µm thick wire.

Tungsten wire has a high strength and is ductile at room temperature (RT). The 150 µm wire has a strength around 3000 MPa increasing up to 4500 MPa for a wire with a diameter of 16 µm [28]. During a tensile test W wire shows a pronounced ductile behaviour expressed in strong necking. The reduction in area is a good measure for the

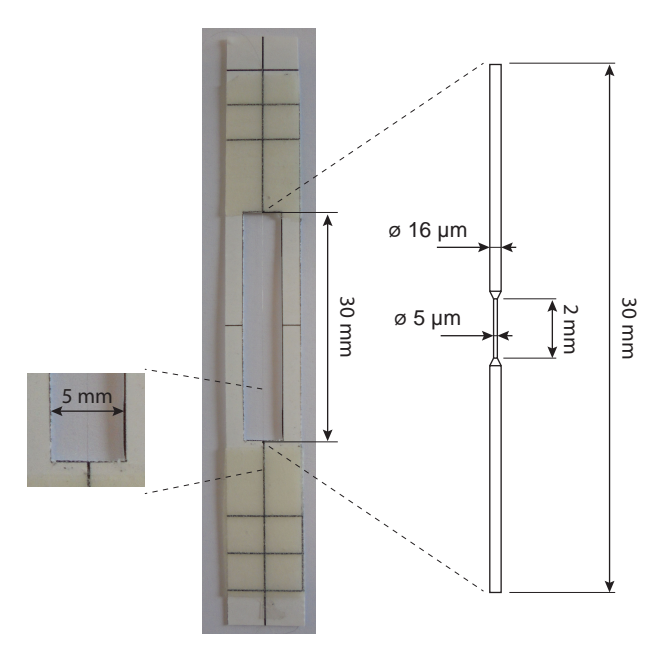


Figure 2. Photo of $16 \,\mu\text{m}$ wire attached to a paper frame by a two component epoxy glue (UHU Plus endfest 300). Extract shows schematically the geometry of the testing area where the centre part is thinned to a diameter of $5 \,\mu\text{m}$ over a length of $2 \,\text{mm}$.

ductility [29]. Tensile tests can therefore not only be used to determine the change in strength directly but also the ductility and its possible reduction by irradiation effects.

Tungsten wire is a standard industrial product originally developed for illumination applications [30]. This ensures the availability of well defined samples with a well controlled quality. Variability in sample quality is thus reduced and a correlation between individual tests is possible.

The as-fabricated fine grained microstructure of a tungsten wire is highly distorted [31, 32]. Due to the drawing process the grains are curled forming the so called van Gogh structure [33]. By annealing the microstructure can be modified in a very controlled way [31, 32]. At moderate temperature the curling as well as most of the dislocations are removed. Although the grain size increases slightly the elongated fine grain structure is maintained. Annealing at high temperature leads to massive grain growth producing few large grains. It can even yield a single grain across the whole diameter.

3. Experimental

Samples were made from potassium doped (60-75 ppm) drawn tungsten wire produced by the OSRAM GmbH, Schwabmünchen. The wire had a nominal diameter of 16 µm and was cut to pieces with a length of 80 - 90 mm, referred to in the following as fibers. For an easier handling the fibres were attached to a paper frame by a two component epoxy glue (UHU Plus endfest 300). In figure 2 a picture of such a frame is shown together with the corresponding dimensions.

Electrochemical thinning was used to reduce the diameter to approximately $5 \,\mu m$ in the centre of the fibre. For that the fibre was coated by an insulating protective lacquer (Plastik70 by Kontakt Chemie) except for a $2 \, mm$ long region in the centre. It was then mounted onto a rotatable sample holder and inserted into an electrolyte (mixture of NaOH (9g), H₂O (300g) and glycerine (450g); details in [34]) for electrochemical thinning. A voltage of $7 \, V$ accompanied by a constant rotation leads to a uniform removal of material in the uncoated area until the target diameter is reached. The length of the thinned area defines the gauge length as due to the ratio of unthinned to thinned area of 10 the fracture will occur in this zone even if a significant increase in strength due to irradiation hardening would occur. Contaminations probably remaining from the fabrication process and/or defects in the lacquer coating, led to inhomogeneities in the thinned area in some cases. The diameter was measured prior to testing by optical microscopy and for selected fibres after fracture at the undeformed part by scanning electron microscopy (SEM).

In total 9 samples were prepared of which 3 samples were used to determine the as-fabricated state and 6 samples were irradiated. For irradiation the samples were irradiated individually in an actively cooled copper sample holder. The thermal contact to the sample holder was ensured by a metal frame (opening 10 mm) and holdingdown pins at both end of the sample (distance 16 mm) respectively. We used a 3 MV tandem accelerator to irradiate the samples with 20.5 MeV W⁶⁺. A fluence of $\Phi_{1\,\mathrm{dpa}}=3.6\times10^{14}\,\mathrm{cm^{-2}}$ produces the damage depth profile shown in figure 3 (a) (as calculated by SRIM). After a first irradiation each sample was manually turned and irradiated again from the opposite side with the same fluence. Assuming a 5 µm wire this leads to the 2d damage profile shown in figure 3 (b) adding up the damage profile from two sides for each line. This is defined as an average damage of 1 dpa. As a consequence of the energy input by the impinging ions the samples are heated. For an approximation we calculate the incoming heat based on ion energy, flux and projected area of the irradiated region. We assume heat conduction to the metal frame or holding down pins (temperature 25°C) and calculate the temperature using Fourier's law. As this is of course only a rough estimation we double checked the results by a finite element calculation using Autodesk Simulation Mechanical 2017 for a medium flux of $3 \times 10^9 \,\mathrm{mm}^{-2} \,\mathrm{s}^{-1}$. The impinging ion energy was modelled as internal heat source as the ions are implanted into the material. Both heat transfer to the supports as well as heat radiation were considered.

The applied damage levels were 0.3 dpa, 1 dpa and 9 dpa respectively. The damage levels were chosen to provide a large spread and correspond to estimated damage levels in a DEMO divertor (10 dpa for a Cu heat sink and 2 dpa for a W armor [35]). The actual ion flux was determined for each irradiation using a Faraday cup. The irradiation time was then adjusted according to this flux and the anticipated damage level. For this study the ion flux varied between 2 and $8 \times 10^9 \,\mathrm{mm}^{-2}\,\mathrm{s}^{-1}$. The values for the individual samples are given in table 1.

The tensile tests were performed with a universal testing machine (TIRA Test 2820)

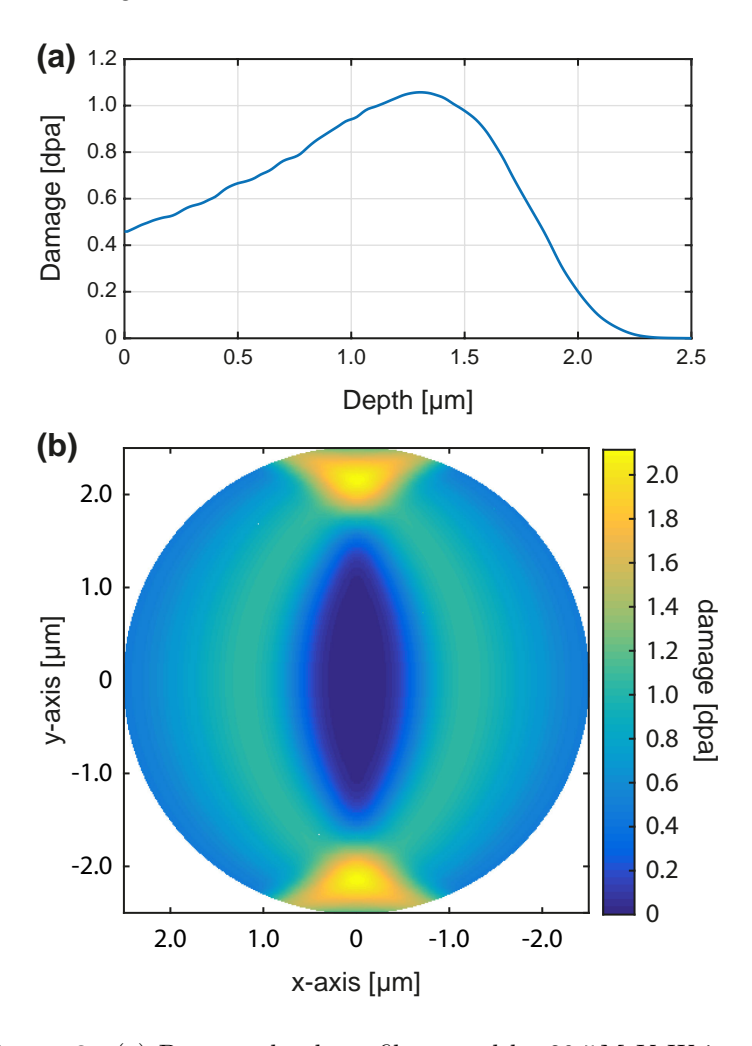


Figure 3. (a) Damage depth profile caused by $20.5\,\mathrm{MeV}$ W ions in W at a fluence of $3.6\times10^{14}\,\mathrm{cm^{-2}}$ calculated by SRIM [23] . (b) Damage profile in a W fibre with a diameter of $5\,\mu\mathrm{m}$ damaged under these conditions at two opposite sides.

at room temperature. A 20 N load cell was used to measure the force in combination with a contact-less optical strain measurement system (details in [28]). In this system the measuring length is defined by chosen reference points which were the transition points to the thinned centre region of the fibres. The tests were performed in a displacement controlled mode with a constant cross-head speed of $0.5 \,\mu m \, s^{-1}$]. After mounting into the testing device the paper frame was cut prior to tensile testing. The samples were preloaded to $5 \, mN$ and aligned using an x-y table.

The fracture surface of all samples was investigated by optical microscopy and for selected samples using a FEI Helios NanoLab 600 scanning electron microscope (SEM). As a measure of deformation, the reduced diameter was determined for selected fibres using the SEM images.

Table 1. Overview of characteristics and test results for the individual irradiated samples. The uncertainty for strength and reduction in area results of the uncertainties in diameter measurements. The ion flux is given as the mean of two irradiations for an individual sample the uncertainty is the standard deviation of the mean of them.

Diameter (measured)	Ion flux	Damage	Beamspot (width x height)	Temperature (esti- mated)	Strength	Reduction of area
$[\mu m]$	$[10^9\mathrm{mm^{-2}s^{-1}}]$	[dpa]	$[\mathrm{mm}^2]$	$[^{\circ}\mathrm{C}]^{'}$	[MPa]	[%]
8.5 ± 0.1	3.4 ± 0.8	0.28	3 x 5	78	4001^{+96}_{-93}	52^{+6}_{-6}
6.6 ± 0.1	2.9 ± 0.7	0.28	3×5	67	4309^{+134}_{-128}	56^{+6}_{-6}
5.7 ± 0.1	2.4 ± 0.4	0.28	3×5	60	4970^{+179}_{-170}	51^{+6}_{-7}
5.4 ± 0.1	2.9 ± 0.8	1.4	3×5	64	3250^{+96}_{-93}	60^{+5}_{-6}
5.4 ± 0.3	8.0 ± 0.3	1.2	2×2	58	3832^{+393}_{-464}	58^{+8}_{-10}
3.8 ± 0.2	8	9.2	2×2	48	3484^{+398}_{-340}	60^{+7}_{-9}

4. Results

In table 1 the detailed characteristics and test results for the irradiated samples are given. The ion flux was calculated as the mean of two opposite sides for each sample. The error is given as the standard deviation of this values. The actual fibre diameters deviate from the projected 5 µm diameter and from each other (compare also figure 5 (c) and (d)). Depending on the actual fluence, beamsize and the used sample holder the calculated temperature varies between 48 and 78 °C. Although two samples have much larger ion flux the temperature is quite similar due to the smaller beamspot. The FEM calculation leads to a maximum temperature of 59 °C.

In figure 4 typical engineering stress-strain curves of non irradiated and ion irradiated samples are shown. In both cases the curves show a clear ductile behaviour with yielding after elastic loading. There is a large scatter in the elastic slope, fracture strain as well as in the strength for the individual irradiation conditions. The strength varies between 3000 and 5000 MPa corresponding to loads between 60 and 100 mN (see table 1 for concrete values). With respect to the uncertainties no clear trend is detectable although the strength seems to decrease rather than increase. A similar trend seems to be valid for the yield point. In figure 5 corresponding fracture surfaces are shown. All fibres show the typical knife-edge fracture and a pronounced necking known for W wire [36, 37]. No difference is visible for nonirradiated and irradiated material.

In table 2 the mean strength and mean reduction in area are summarized. For comparison also the value for a non irradiated $16 \,\mu m$ wire is given (taken from [28]). The mean strength increases for 0.3 dpa and decreases afterwards but at the same time shows a large error. The reduction in area shows a very small spread and lies between 50 and $60\,\%$.

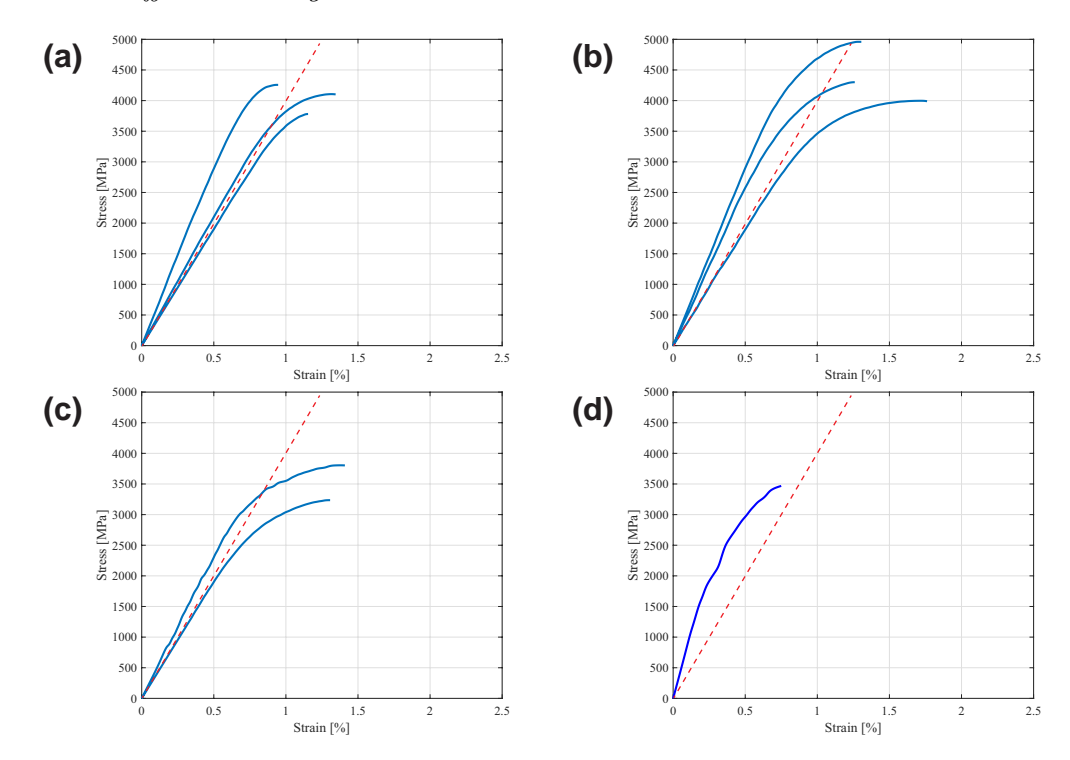


Figure 4. Stress-strain curve of tensile tested drawn tungsten wire with a nominal diameter of $5\,\mu\mathrm{m}$ in (a) initial state and after irradiation to (b) $0.3\,\mathrm{dpa}$, (c) 1 dpa and (d) 9 dpa. The curves were adjusted in a way that the elastic line starts in the origin and smoothed by a cubic smoothing spline (MATLAB function: "'smoothingspline"'). After elastic loading all samples show yielding and distinct plastic behaviour. The red dashed lines indicate an elastic deformation corresponding to a Young's modulus of $400\,\mathrm{GPa}$

Table 2. Summary of tensile test results calculated as the weighted mean. For comparison the value for 16 μm wire is given (taken from [28].

Nominal	Damage	Strength	Reduction in area
$diameter \ [\mu m]$	[dpa]	[MPa]	[%]
16		4481 ± 35	49 ± 1
5	-	4077 ± 71	55 ± 3
5	0.3	4245 ± 70	53 ± 4
5	1	3302 ± 115	60 ± 5
5	9	3484^{1}	60^{1}

¹⁾ only one valid test

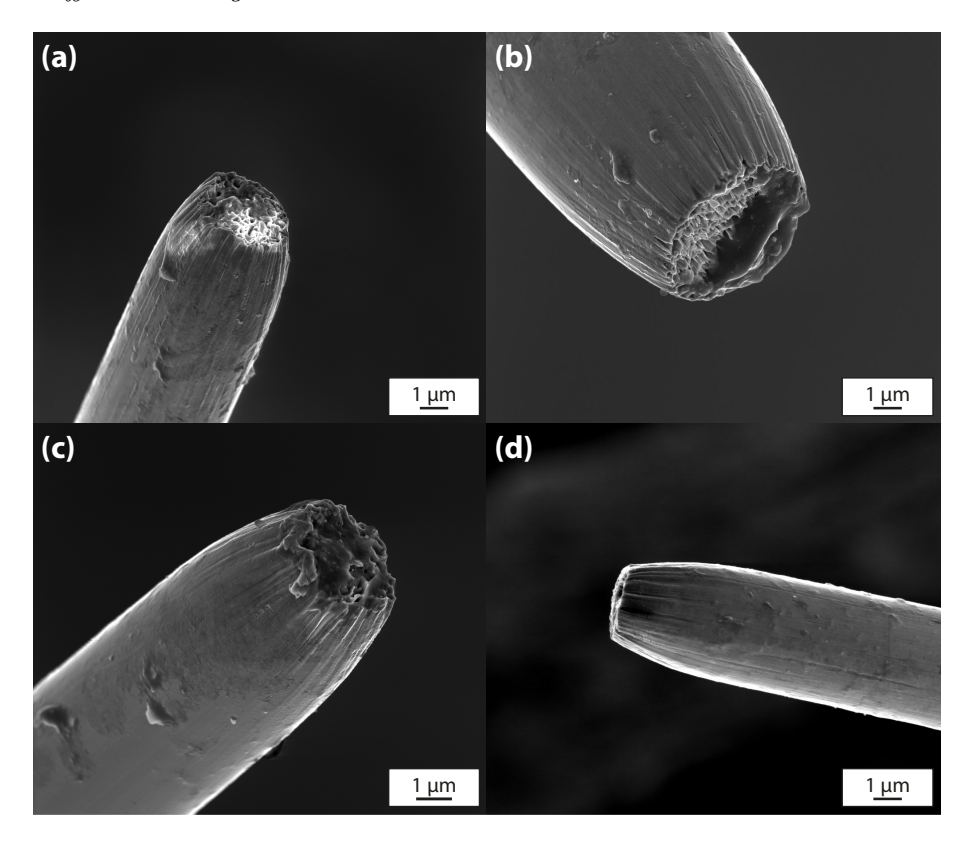


Figure 5. Fracture surface of tensile tested drawn tungsten wire with a diameter of 5 µm in (a) non irradiated state and after irradiation to (b) 0.3 dpa, (c) 1 dpa and (d) 9 dpa. All samples show pronounced necking.

5. Discussion

5.1. Measuring technique

Sample preparation by electropolishing allows a reduction of the diameter to the necessary dimension but the uniformity as well as the controllability (final diameter) is limited at the moment. The influence of the diameter variations is expected to be low strength and reduction in diameter as both is defined by the thinnest region. However, there is probably an effect on the strain measurement which could be a reason for the strong variations seen in the stress-strain curves (see figure 4). For example a variation of the mean diameter of only 5% would explain the deviation of the Young's Modulus in figure 4 (d). The large beam size ensures the full irradiation of the sample and minimizes the risk of miss alignment. However, as the beam shows a gaussian ditribution a variation in the damage level along the fibre might still be present. A beam scanning along the fibre axis should be used to avoid this problem in the future. Calculations show that the sample only reaches moderate temperatures below 100 °C (compare table 1). Even assuming a bad thermal contact, e.g. by isolating epoxy resulting from sample preparation, the temperature would only reaches 120 °C as calculated by the FEM model. This temperature region is far from a temperature where significant annihilation

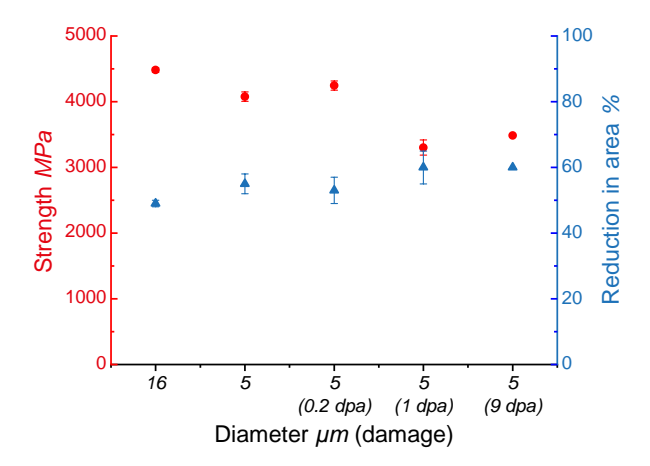


Figure 6. Overview of strength (red squares) and reduction in area (blue triangles) for tungsten wire with a diameter of $16 \, \mu m$ and $5 \, \mu m$ in the as fabricated case and for tungsten wire with a diameter of $5 \, \mu m$ after irradiation. Bottom line indicates diameter and damage level in brackets.

of irradiation defects is expected as for ion irradiated tungsten only at a temperature of $1400\,^{\circ}\mathrm{C}$ all defects vanished [38] . The very small load (depending on the diameter between 40 and $260\,\mathrm{mN}$) and strain values put difficulties in quantitative measurements. Whereas a optimized load cell would give some improvement a strain measuring system specifically designed for the small scale samples would be very beneficial. The presented procedure only alloys sequential investigations. Simultaneous irradiation and loading could lead to different results due to synergistic effects as reported for H retention . Having an in-situ testing capability would in addition lower the risk of damaging the fragile samples during transfer.

5.2. Conservation of ductility

All samples showed a ductile behaviour irrespective of the damage level. This can clearly be seen in the fracture surface (see figure 5) as well as in the yielding visible in the stress strain curves (see figure 4). In figure 6 an overview of the strength and reduction in area is given. There is a moderate decrease in strength with increasing damage level and thus no sign of irradiation hardening. The reduction in area stays more or less constant and even shows a slight increase. If considering it as a measure for ductility there is no reduction of ductility detectable.

It has to be noted that uncertainties in the diameter measurement have a large influence on the stress values (quadratic dependence) and thus complicate quantitative statements about hardening. However, hardening typically observed for tungsten goes up to 34 % for ion irradiated tungsten [25] and up to 100 % for neutron irradiated samples [39] which should also be well visible in strength values. Regarding ductility it has to be considered that the brittle to ductile transition (BDT) of the tungsten wire is well below RT (DBT of wire with a diameter of 250 μ m is around -100°) [40]. Therefore embrittlement shown by an increase in BDT could not have been detected as long as this

increase has not reached RT. Measurements of the BDT of as-fabricated and irradiated samples are planned. However, BDT shifts of 600 °C have been observed for tungsten irradiated to 1 dpa in a fission reactor [41].

The irradiation of the sample is not uniform and most of the samples are thicker than the desired 5 µm. However, due to the circular shape the non irradiated area is low (for the sample with 8.5 µm the non irradiated centre is only 20% assuming a penetration of 2.5 µm). The sample with highest damage rate does show a lower strength compared to the non irradiated case although it is also the thinnest sample. Therefore, we assume that the diameter variation does not conceal irradiation hardening. Nevertheless, a direct detection of the irradiation damage in the microstructure would be very helpful to get an idea about the uniformity. Due to the already very distorted microstructure in the as-fabricated condition (see figure 1) the detection of damage is challenging. Transmission electron microscopy (TEM) is planned for as-fabricated and irradiated material. In addition gentle heat treatment before irradiation can help to reduce the defect density in the as fabricated case (see e.g. [31, 32]) and allow for an easier detection of irradiation caused damage.

Typically bulk tungsten shows distinct irradiation hardening (see above) and loss of ductility. It is known that irradiation effects is not so pronounced in highly deformed and very fine grained material [42]. In the case of tungsten sheet material Armstrong et al. [43] attributed this to the recombination of irradiation caused point defects on subgrains which are caused by the high dislocation density. This is probably also true for the thin W wire as also the wire has a very fine microstructure (see figure 1).

Furthermore, w wire, although featuring a very high dislocation density, exhibits distinct ductile deformability as e.g. shown in [31] for as-fabricated wire having a highly distorted micro-structure but still behave ductile. Whether this does mean that the deformation mechanism active in W wire is also less affected by defects induced by irradiation needs further investigation .

5.3. Consequences for the use in tungsten fibre-reinforced composites

In the case of W_f/W the properties of the composite are dominated by the properties of the used wire [44]. This also refers to the indirect influence by the activation of extrinsic toughening mechanisms e.g. a ductile fibre leads to ductile failure, a brittle fibre rather to pull-out. Investigations on the tungsten wire can therefore be used for models describing the composite behaviour. At the moment, mainly wire with a diameter of 150 µm is used in W_f/W . The use of thinner wires down to a diameter of 16 µm is envisaged [45]. In [28] it was shown that the mechanical behaviour 150 µm wire is very similar to the thin wire. This means that even now the presented approach will help predicting the irradiation behaviour of W_f/W . The studies will be even more relevant once the thin wire is used in the composites. The observed conservation of the ductility would be very beneficial for the composite behaviour as the ductile deformation is a very effective mechanism for toughening [29]. In addition, due to the missing embrittlement

the stregth of the wire is preserved which is especially favorable for W_f/Cu.

85 6. Concluding remarks and outlook

Despite a very challanging experimental procedure, the used test method allowed successful tensile testing and thus the determination of mechanical properties of the thin tungsten wire which was fully irradiated by high energetic ions. With technique a systematic study of irradiation effects on the mechanical properties of thin W wire is now possible. In addition this opens possibilities for the further development of tungsten based composites.

It is planned to increase the number of tests and the dose rate to increase the statistical relevevance of the results. To allow synergistic studies a tensile testing rig allowing mechanical tests in combination with ion beam loading will be developed. Here the focus must also lie in an optimized experimental setup e.g. a low load sensitive load cell and an improved direct strain measurement.

7. Acknowledgments

This work has been carried out within the framework of the EUROfusion Consortium and has received funding from the Euratom research and training programme 2014-2018 and 2019-2020 under grant agreement No 633053. The views and opinions expressed herein do not necessarily reflect those of the European Commission.

References

305

310

315

320

- [1] Federici G, Bachmann C, Barucca L, Baylard C, Biel W, Boccaccini L V, Bustreo C, Ciattaglia S, Cismondi F, Corato V, Day C, Diegele E, Franke T, Gaio E, Gliss C, Haertl T, Ibarra A, Holden J, Keech G, Kembleton R, Loving A, Maviglia F, Morris J, Meszaros B, Moscato I, Pintsuk G, Siccinio M, Taylor N, Tran M Q, Vorpahl C, Walden H and You J H 2019 Nuclear Fusion 59 066013
- [2] Coenen J W, Antusch S, Aumann M, Biel W, Du J, Engels J, Heuer S, Houben A, Hoeschen T, Jasper B, Koch F, Linke J, Litnovsky A, Mao Y, Neu R, Pintsuk G, Riesch J, Rasinski M, Reiser J, Rieth M, Terra A, Unterberg B, Weber T, Wegener T, You J H and Linsmeier C 2016 Physica Scripta T167 014002
- [3] Federici G, Biel W, Gilbert M R, Kemp R, Taylor N and Wenninger R 2017 Nuclear Fusion 57 092002
- [4] Yih S W and Wang C T 1979 Tungsten: Sources, Metallurgy, Properties, and Applications (New York: Plenum Press)
- [5] Steichen J 1976 Journal of Nuclear Materials 60 13–19
- [6] Maloy S A, James M R, Sommer W, Willcutt G J, Lopez M, Romero T J and Toloczko M B 2005 Journal of Nuclear Materials 343 219–226
- [7] Zinkle S J 2016 Physica Scripta **T167** 014004
- [8] Linsmeier C, Rieth M, Aktaa J, Chikada T, Hoffmann A, Hoffmann J, Houben A, Kurishita H, Jin X, Li M, Litnovsky A, Matsuo S, von Mueller A, Nikolic V, Palacios T, Pippan R, Qu D, Reiser J, Riesch J, Shikama T, Stieglitz R, Weber T, Wurster S, You J H and Zhou Z 2017 Nuclear Fusion 57

330

335

340

355

365

- [9] Riesch J, Han Y, Almanstötter J, Coenen J W, Höschen T, Jasper B, Zhao P, Linsmeier C and Neu R 2016 *Physica Scripta* **T167** 014006
- [10] Mao Y, Coenen J W, Riesch J, Sistla S, Almanstötter J, Reiser J, Terra A, Chen C, Wu Y, Raumann L, Höschen T, Gietl H, Neu R, Linsmeier C and Broeckmann C 2019 Nuclear Fusion 59 086034
- [11] Gietl H, Olbrich S, Riesch J, Holzner G, Höschen T, Coenen J W and Neu R 2020 Engineering
 Fracture Mechanics 232 107011
- [12] Chawla K K 1993 Ceramic Matrix Composites (Boston, MA: Springer US) ISBN 978-1-4757-2216-1
- [13] Müller A, Ewert D, Galatanu A, Milwich M, Neu R, Pastor J Y, Siefken U, Tejado E and You J H 2017 Fusion Engineering and Design 124 455–459
- [14] Müller A V, Böswirth B, Cerri V, Greuner H, Neu R, Siefken U, Visca E and You J H 2020 Physica Scripta T171 014015
- [15] Zinkle S J and Busby J T 2009 Materials Today 12 12–19
- [16] Was G S 2017 Fundamentals of Radiation Materials Science: Metals and Alloys 2nd ed (New York, NY and s.l.: Springer New York) ISBN 9781493934362
- [17] Markelj S, Schwarz-Selinger T, Pečovnik M, Založnik A, Kelemen M, Čadež I, Bauer J, Pelicon P, Chromiński W and Ciupinski L 2019 Nuclear Fusion 59 086050
- [18] Gilbert M R and Sublet J C 2011 Nuclear Fusion 51 043005
- [19] Hasegawa A, Fukuda M, Yabuuchi K and Nogami S 2016 Journal of Nuclear Materials 471 175– 183
- [20] Das S 2019 SN Applied Sciences 1
- [21] Was G S and Averback R S 2011 Radiation damage using ion beams Comprehensive Nuclear Materials ed Konings R (Burlington: Elsevier Science) pp 195–221 ISBN 9780080560335
 - [22] Mahmood T, Griffiths M, Lemaignan C and Adamson R Material test reactors and other irradiation facilities URL https://www.antinternational.com/docs/samples/FM/11/ZIRAT23_STR_Material_Test\-_Reactors_and_other_Irradiation_Facilities_Sample.pdf
- 230 [23] Ziegler J and Biersack J Srim: The stopping range of ions in matter URL http://www.srim.org
 - [24] Wielunska B, Mayer M, Schwarz-Selinger T, Sand A and Jacob W 2020 Nuclear Fusion 60 096002
 - [25] Armstrong D, Hardie C D, Gibson J, Bushby A J, Edmondson P D and Roberts S G 2015 Journal of Nuclear Materials 462 374–381
 - [26] Prasitthipayong A 2017 Small-Scale Mechanical Testing and Size Effects in Extreme Environments
 Ph.D. thesis University of California Berkeley URL https://escholarship.org/uc/item/
 6sc4c0z8#main
 - [27] Hosemann P, Shin C and Kiener D 2015 Journal of Materials Research 30 1231–1245
 - [28] Riesch J, Feichtmayer A, Fuhr M, Almanstötter J, Coenen J W, Gietl H, Höschen T, Linsmeier C and Neu R 2017 Physica Scripta T170 014032
 - [29] Riesch J, Almanstötter J, Coenen J W, Fuhr M, Gietl H, Han Y, Höschen T, Linsmeier C, Travitzky N, Zhao P and Neu R 2016 IOP Conference Series: Materials Science and Engineering 139 012043
 - [30] Schade P 2010 International Journal of Refractory Metals and Hard Materials 28 648–660
 - [31] Zhao P, Riesch J, Höschen T, Almanstötter J, Balden M, Coenen J W, Himml R, Pantleon W, von Toussaint U and Neu R 2017 International Journal of Refractory Metals and Hard Materials 68 29–40
 - [32] Nikolić V, Riesch J, Pfeifenberger M J and Pippan R 2018 Materials Science and Engineering: A 737 434–447
 - [33] Hosford W F 1964 Transaction of the Metallurgical Society of AIME 12–15
 - [34] Manhard A, von Toussaint U, Balden M, Elgeti S, Schwarz-Selinger T, Gao L, Kapser S, Płociński T, Grzonka J, Gloc M and Ciupiński Ł 2017 Nuclear Materials and Energy 12 714–719
 - [35] You J H, Mazzone G, Visca E, Bachmann C, Autissier E, Barrett T, Cocilovo, Crescenzi F, Domalapally P K, Dongiovanni, Entler S, Federici G, Frosi P, Fursdon M, Greuner H, Hancock, Marzullo, McIntosh S, Müller A V, Porfiri M T, Ramogida G, Reiser J, Richou M, Rieth M,

- Rydzy A, Villari R and Widak 2016 Fusion Engineering and Design 109-111 1598-1603
- [36] Leber S, Tavernelli J, White D D and Hehemann R F 1976 Journal of the Less Common Metals 48 119–133
- [37] Terentyev D, Tanure L, Bakaeva A, Dubinko A, Nikolić V, Riesch J, Verbeken K, Lebediev S and Zhurkin E E 2019 International Journal of Refractory Metals and Hard Materials 81 253–271
- [38] Ferroni F, Yi X, Arakawa K, Fitzgerald S P, Edmondson P D and Roberts S G 2015 Acta Materialia 90 380–393
 - [39] Miyazawa T, Garrison L M, Geringer J W, Fukuda M, Katoh Y, Hinoki T and Hasegawa A 2020 Journal of Nuclear Materials 529 151910
 - [40] Seigle L L and Dickinson C D 1963 Refractory Metals and Alloys II 17 65–116
 - [41] Gaganidze E, Chauhan A, Schneider H C, Terentyev D, Borghmans G and Aktaa J 2021 Journal of Nuclear Materials **547** 152761
 - [42] Beyerlein I J, Caro A, Demkowicz M J, Mara N A, Misra A and Uberuaga B P 2013 Materials Today 16 443–449
 - [43] Armstrong D E and Britton T B 2014 Materials Science and Engineering: A 611 388–393
- [44] Gietl H, Riesch J, Coenen J W, Höschen T, Linsmeier C and Neu R 2017 Fusion Engineering and Design 124 396–400
 - [45] Gietl H, Müller A V, Coenen J W, Decius M, Ewert D, Höschen T, Huber P, Milwich M, Riesch J and Neu R 2018 Journal of Composite Materials 52 3875–3884